

Comparisons of Co-Seismic Gravity Changes between GRACE Observations and the Predictions from the Finite-Fault Models for the 2012 Mw = 8.6 Indian Ocean Earthquake Off-Sumatra

Armin Rahimi

Abstract—The Gravity Recovery and Climate Experiment (GRACE) has been a very successful project in determining mass redistribution within the Earth system. Large deformations caused by earthquakes are in the high frequency band. Unfortunately, GRACE is only capable to provide reliable estimate at the low-to-medium frequency band for the gravitational changes. In this study, we computed the gravity changes after the 2012 Mw8.6 Indian Ocean earthquake off-Sumatra using the GRACE Level-2 monthly spherical harmonic (SH) solutions released by the University of Texas Center for Space Research (UTCSR). Moreover, we calculated gravity changes using different fault models derived from teleseismic data. The model predictions showed non-negligible discrepancies in gravity changes. However, after removing high-frequency signals, using Gaussian filtering 350 km commensurable GRACE spatial resolution, the discrepancies vanished, and the spatial patterns of total gravity changes predicted from all slip models became similar at the spatial resolution attainable by GRACE observations, and predicted-gravity changes were consistent with the GRACE-detected gravity changes. Nevertheless, the fault models, in which give different slip amplitudes, proportionally lead to different amplitude in the predicted gravity changes.

Keywords—Undersea earthquake, GRACE observation, gravity change, dislocation model, slip distribution.

I. INTRODUCTION

THE April 11, 2012, Mw8.6 earthquake off the west coast of northern Sumatra, Indonesia, hit in a couple of hours by the largest strike-slip earthquake ever recorded within the oceanic lithosphere of the Indo-Australia plate. Broadband seismological observations of the Mw8.6 main-shock indicate a large centroid depth (30 km) and remarkable rupture complexity [1].

Reliable estimation of co-seismic earthquake slip is essential to evaluate the pre-locking status and the level of stress release. However, existing slip models obtained by various constraints or via inversion of observations exhibit notable differences. Data from teleseismic networks have been used to observe and model the co-seismic signature and slip history of the Indian earthquake [2]-[5]. Different scenarios have been proposed for this earthquake. Reference [2] proposed a left lateral strike-slip fault trending north-northeast

to south-southwest with maximum slip of 35 meters by using 31 teleseismic P waveforms (model-a). Reference [3] analyzed 28 teleseismic broadband P waveforms, 27 broadband SH waveforms, and 45 long period surface waves. The fault they proposed has the same direction (strike=20) as [2], while it has maximum slip of 55 meters (model-b). Reference [4] analyzed 38 teleseismic broadband P waveforms, 13 broadband SH waveforms, and 56 long period surface waves. They released two fault slip distribution models. The first model (model-c) proposed by them has approximately the same orientation as [2] and [3], while it was a right lateral strike-slip fault with 70 meters maximum slip. The second fault model (model-d) has a distinctly different orientation with the first model with a maximum slip of 55 meters. Reference [5] used seismic wave analyses to reveal that the 11 April 2012 event had an extra ordinarily complex four-fault rupture (model-e). The main-shock rupture on a right-lateral strike slip fault trending west-northwest to east-southeast (WNW-ESE) with maximum slip of 30 meters, and then another rupture was triggered on an orthogonal left lateral strike-slip fault trending north-northeast (NNE-SSW) to south-southwest that crosses the first fault. This was followed by westward rupture on a second WNW-ESE strike-slip fault offset about 150 kilometers towards the southwest from the first fault. Finally, rupture was triggered on another WNW-ESE fault about 330 kilometers west of the epicenter. Figs. 1 and 2 show location and slip distribution of mentioned faults.

Tables I and II compare some key parameters. As can be seen from these tables, not only are there discrepancies in the length and width of the fault plane, but also there are different fault orientations. The difference in the predicted maximum slip between the five models is as large as 30 meters, and the difference in the fault depth ranges up to 9 kilometers. Moreover, the slip distributions predicted by these models have large discrepancies.

The fault models for the Indian Ocean earthquake have non-negligible discrepancies. The discrepancies can be attributed to the lack of amount of data due to measurement limits on ocean in comparison with earthquakes hit on land for which other source of data provide better constrains. In addition to teleseismic data, spaceborne gravimetry data from GRACE have been used to observe the co-seismic and post-seismic signature of the 11 April 2012 Mw = 8.6 Indian Ocean earthquake [6], [7]. Moreover, fault parameter inversion using

Armin Rahimi is with the Geodesy Division, Department of Surveying and Geomatic Engineering, College of Engineering, University of Tehran, Tehran, Iran (e-mail: armin_rahimi@ut.ac.ir).

GRACE data based on multiple centroid moment tensors and normal mode formulation have been demonstrated for a number of large earthquakes include Indian Ocean earthquake over the last decade [6]. In this study, we compare co-seismic

gravity changes between GRACE observations and the predictions from the mentioned finite-fault models for the 2012 Mw = 8.6 Indian Ocean earthquake off-Sumatra.

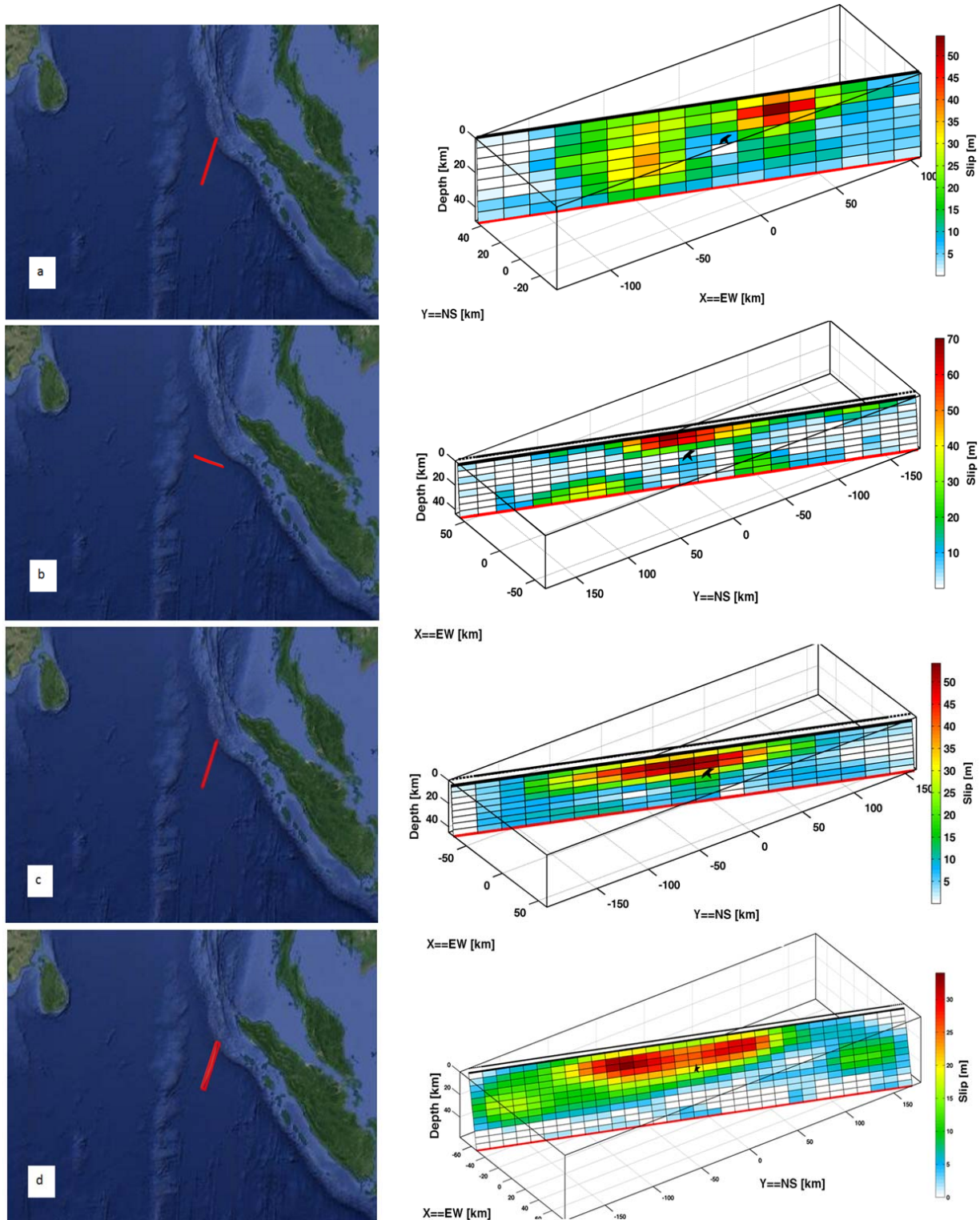


Fig. 1 The slip models a-d

II. DATA AND METHODS

To compute gravity change corresponding to the 2012 Mw8.6 Indian Ocean earthquake off-Sumatra, we use monthly GRACE gravity solutions of Level-2 (RL05) products from the UTCSR. The C20 coefficients are replaced by satellite laser ranging (SLR) estimates [8].

To suppress seasonal variations and separate co-seismic change, we subtract two mean gravity field after and before the earthquake which is known as stacking approach based on that from [9]. In order to reduce striping errors we use Gaussian 350km filter. In the SH domain, Gaussian smoothing is to apply a weight to each SH coefficient differences [10], [11]. The difference of SH coefficients ΔC_{lm} , ΔS_{lm} of each monthly field are then used to compute gravity change.

The gravity change Δg is given by:

$$\Delta g(\theta, \lambda) = \sum_{l=0}^N \frac{GM}{R^2} (l-1)$$

$$\sum_{m=0}^l \bar{P}_{lm}(\cos \theta)(\Delta C_{lm} \cos m\lambda + \Delta S_{lm} \sin m\lambda)$$

where θ and λ are colatitude and longitude and \bar{P}_{lm} is normalized associated Legendre function. What is more, this difference include post-seismic signals related earthquake. So, to eliminate the mentioned effects in the GRACE observations, first, we adopt at a $1^\circ \times 1^\circ$ grid a time-dependent function [12].

$$y(t) = a + b(1 - e^{-t/\tau})$$

where a is constant term, τ and b are the relaxation time and total post-seismic gravitational gradient change at end of the relaxation.

Fig. 3 (a) shows observed gravity changes computed by differencing the two year mean field before and after the earthquake in which consist of both co-seismic and post-seismic signals. Fig. 3 (b) shows the post-seismic gravity changes by time series fitting. Fig. 3 (c) shows co-seismic gravity change, computed by removing post-seismic effects.

TABLE I
COMPARISONS OF KEY CHARACTERISTICS IN THE FINITE-FAULT

| Model | Length (km) | Width (km) | Depth (km) | Strike (deg.) | Dip (deg.) | Rake (deg.) | Max slip(m) | Magnitude (Mw) | Latitude | Longitude |
|-------|-------------|------------|------------|---------------|------------|-------------|-------------|----------------|----------|-----------|
| a | 375.00 | 40.00 | 21.36 | 198.87 | 79.95 | 360.04 | 70 | 8.56 | 2.3658 | 93.0812 |
| b | 255.00 | 48.00 | 21.00 | 108.34 | 86.98 | 172.30 | 55 | 8.56 | 2.3554 | 93.0545 |
| c | 380.00 | 40.00 | 22.90 | 20.00 | 80.00 | 358.19 | 55 | 8.64 | 2.3100 | 93.0600 |
| d | 384.00 | 60.00 | 22 | 20.00 | 64.00 | 1.00 | 35 | 8.57 | 2.3110 | 93.0630 |

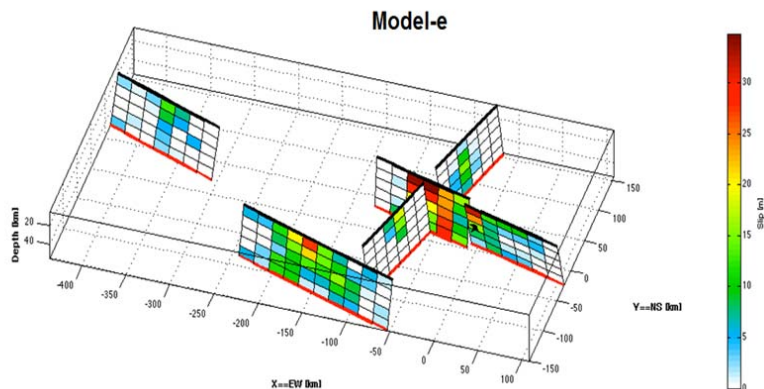
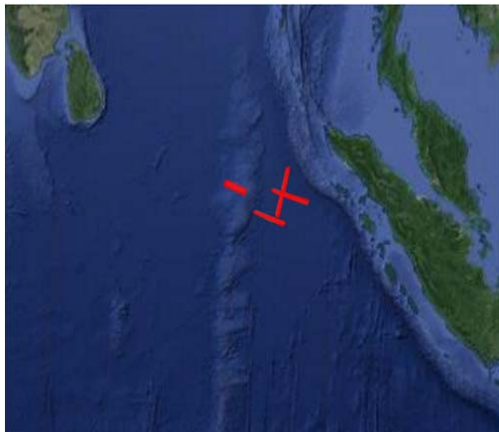


Fig. 2 The slip model-e

TABLE II
KEY PARAMETERS OF MODEL-E

| Model-e | Length | Width | Depth | Strike (deg.) | Dip (deg.) | Rake (deg.) | Max slip(m) | Magnitude (Mw) | Rupture time(s) |
|---------|--------|-------|-------|---------------|------------|-------------|-------------|----------------|-----------------|
| A | 120 | 50 | 30 | 106 | 75 | 185 | 37 | 8.54 | 0 |
| B | 130 | 50 | 30 | 106 | 75 | 185 | 37 | | |
| C | 120 | 50 | 30 | 16 | 80 | 370 | 11 | 7.94 | 30 |
| D | 130 | 50 | 30 | 16 | 80 | 370 | 11 | | 70 |
| E | 200 | 50 | 30 | 109 | 80 | 180 | 26 | 8.3 | 60 |
| F | 150 | 50 | 30 | 111 | 74 | 180 | 12 | 7.84 | 110 |

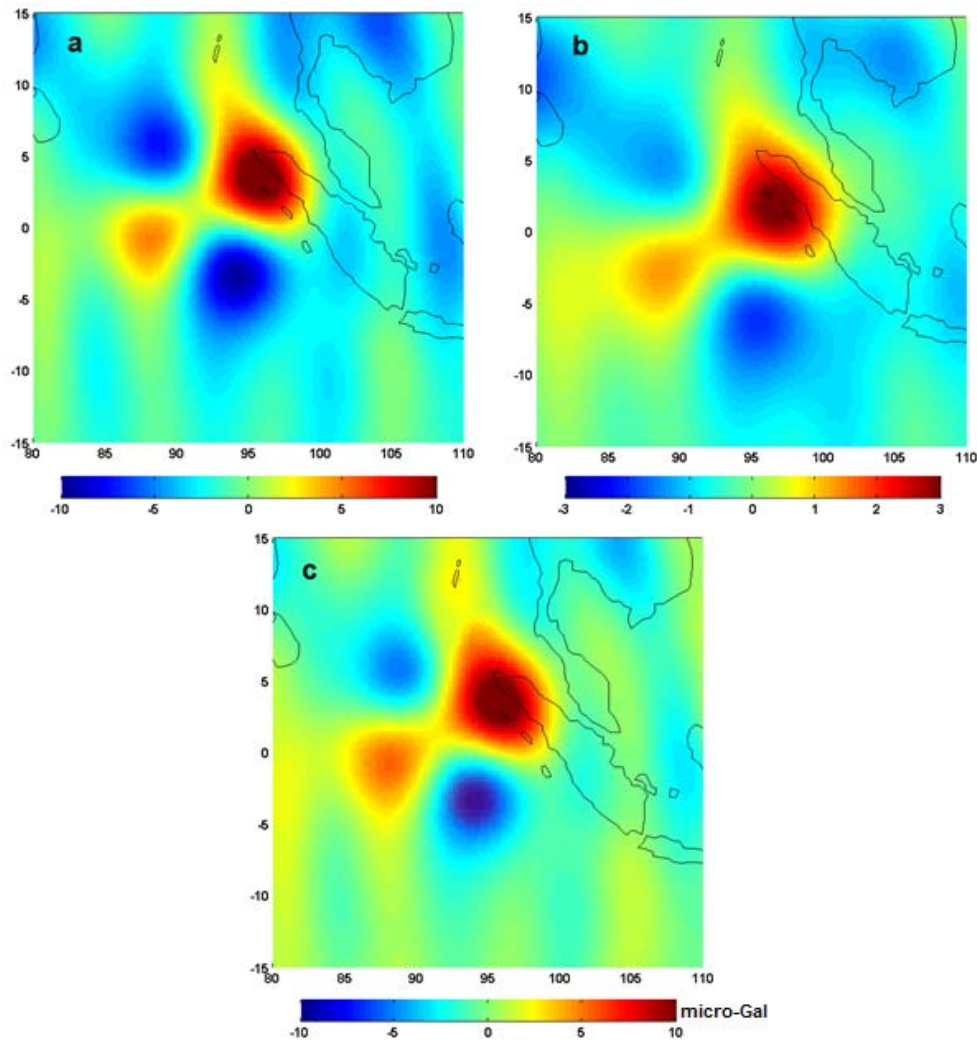


Fig. 3 (a) The GRACE observed gravity changes due to the 2012 Indian Ocean earthquakes is computed by differencing the 2 year mean field before and after the earthquake in which consist of both co-seismic and post-seismic signals. (b) The post-seismic gravity changes by time series fitting (c) The co-seismic GRACE gravity change is computed by subtracting a and b

TABLE III
THE 7-LAYERED HALF-SPACE MODEL OF INDIAN OCEAN MW 8.6 EARTHQUAKE (THE PARAMETERS ARE FROM CRUST 2.0)

| layer | Depth(km) | vp[km/s] | vs[km/s] | ρ [kg/m ³] | Viscosity (10 ¹⁹ Pa s) | material |
|-------|-----------|----------|----------|-----------------------------|-----------------------------------|--------------|
| 1 | 0 | 5.79 | 3.19 | 2600 | ∞ | Elastic body |
| 2 | 15.00 | 6.79 | 3.89 | 2900 | ∞ | Elastic body |
| 3 | 24.40 | 8.1 | 4.48 | 3380 | ∞ | Elastic body |
| 4 | 40.00 | 8.09 | 4.47 | 3380 | ∞ | Elastic body |
| 5 | 60.00 | 8.08 | 4.46 | 3380 | ∞ | Elastic body |
| 6 | 80.00 | 8.00 | 4.38 | 3370 | ∞ | Elastic body |
| 7 | 115.00 | 7.98 | 4.36 | 3370 | 1 | Maxwell body |

In order to predict gravity changes, we use the FORTRAN code PSGRN/PSCMP provided by [13], which is based on a semi-analytical approach for a layered half-space [13]. The five mentioned fault slip models and the 7-layered half-space model (Table III) based on the CRUST2 seismic velocity models [14] are used as input.

We compute the co-seismic gravity field variations in a $10^\circ \times 10^\circ$ region with cell size of $0.3^\circ \times 0.3^\circ$ commensurate with the local distribution of GRACE. The model-predicted gravity variation is the result at the space-fixed point, which does not contain the free air correction caused by the vertical displacement on the earth's surface [15]. The space-fixed point gravity variations are consistent with GRACE results, as

the satellites in space do not ‘see’ this air correction term on the deformed earth surface [16]. Moreover, the dislocation theory above is assumed dry earth, so the deformation that occurred in the ocean bottom is replaced by sea water, because of the sea bottom displacement causes additional potential and gravity changes. The correction can be done by a Bouguer layer reduction [17], [18].

$$\delta g^{w.c.} = -2\pi G \rho_w \Delta h$$

where G denotes the Newton’s gravitational constant, $\rho_w = 1.03 \text{ gcm}^{-3}$ represents the sea water density and Δh is the co-seismic vertical displacement.

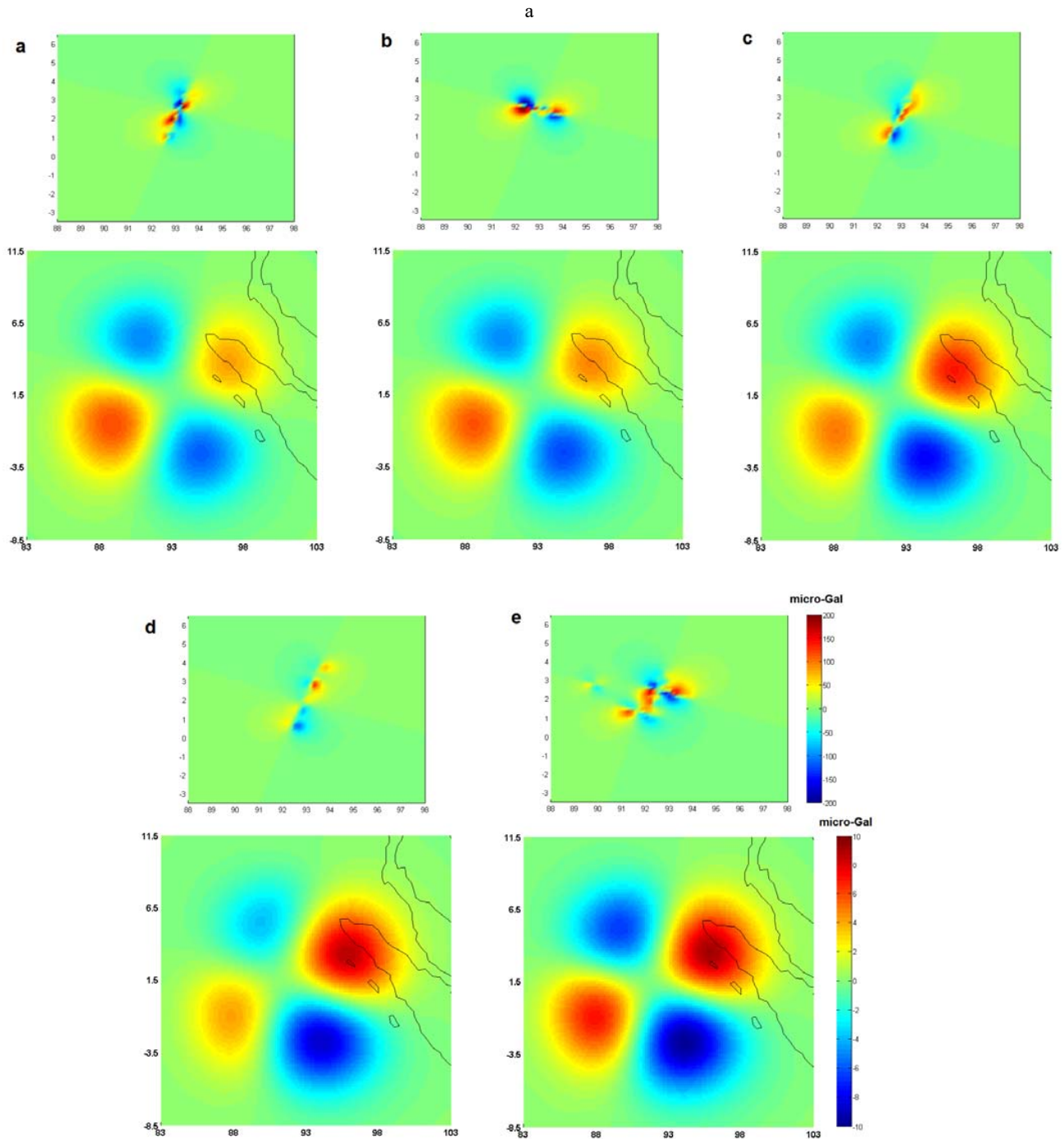


Fig. 4 Predicted gravity change on space-fixed point with and without Gaussian filter 350 km: (a) model-a; (b) model-b; (c) model-c; (d) model-d; (e) model-e

The amplitude and spatial distribution mode of the predicted gravity field variations differ significantly from the corresponding GRACE results because of the limited spatial resolution of GRACE. The GRACE satellites are known sensitive only to the low-frequency gravity change due to the attenuation of the signals. To obtain a comparable spatial resolution in the model-predicted gravity field variations, we express the regional distributions as the SH coefficients to degree of 60 and adopt 350 km Gaussian. According to Fig. 4, the predicted gravity changes of five slip models before applying Gaussian filter are distinctly different while after applying Gaussian filter, the spatial patterns of total gravity change predicted from all five slip models become similar at the spatial resolution attainable by GRACE observations, and consistent with the GRACE-detected gravity changes (Fig. 3 (c)). By applying Gaussian filter we remove high-frequency signals because GRACE has a limited spatial resolution of several hundreds of kilometers, while gravity changes predicted by dislocation models contain short-wavelength signals. Moreover, we show GRACE observations are not sensitive to slip distribution and orientation of fault. For instance, although model-a and model-b (Figs. 1 (a) and (b)) not only have different slip distribution but also have different orientation, the predicted gravity changes after applying Gaussian has the same amplitude and spatial pattern. However, the gravity changes of both slip models before applying Gaussian reveal rupture line consistent with fault

orientation. Therefore, the applications of spaceborne gravimetry to earthquake studies are seriously limited by low spatial resolution, mainly because the length of faulting is of the same order of magnitude as the limiting resolution of the GRACE data.

The amplitudes from the five models are discernibly different. Since the five models give different slip amplitudes, they proportionally lead to different amplitude in the predicted co-seismic gravity change. Peak values in the negative signals predicted by Models a–e are -4.1 micro-Gal, -5.2 micro-Gal, -7.3 micro-Gal and -9.8 micro-Gal, respectively (Fig. 4). Similarly, reference [19] shows that models with different slip amplitudes, lead to different amplitude in the predicted co-seismic gravity changes and they conclude that the GRACE-derived amplitudes can be used to independently constrain the fault parameters of the Maule earthquake, since these are discernibly different from the amplitudes derived by other co-seismic slip models. Although all Models are derived from teleseismic wave analysis, the maximum slip amplitudes are range from 37m to 70m, presumably because of different model assumptions and data distributions, as well as different intrinsic ranges of apparent velocities in the observations [4].

GRACE-detected gravity changes are compared with model predictions on two profiles along latitudes 6 N and 1.5 S (Figs. 5 and 6). Among the five slip models the predicted gravity changes of the model-e is closer to GRACE-detected gravity changes which can be seen in Figs. 5 and 6.

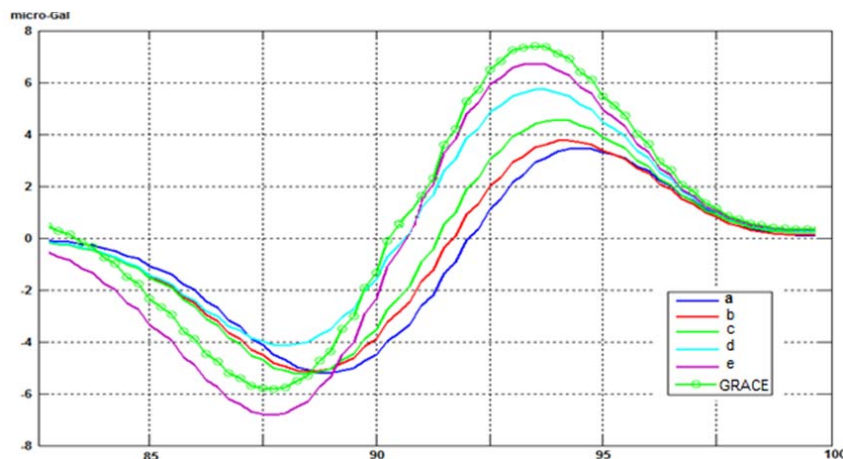


Fig. 5 Comparisons of co-seismic gravity changes for the profiles along 6 N between GRACE observations and the predictions from the five finite-fault models

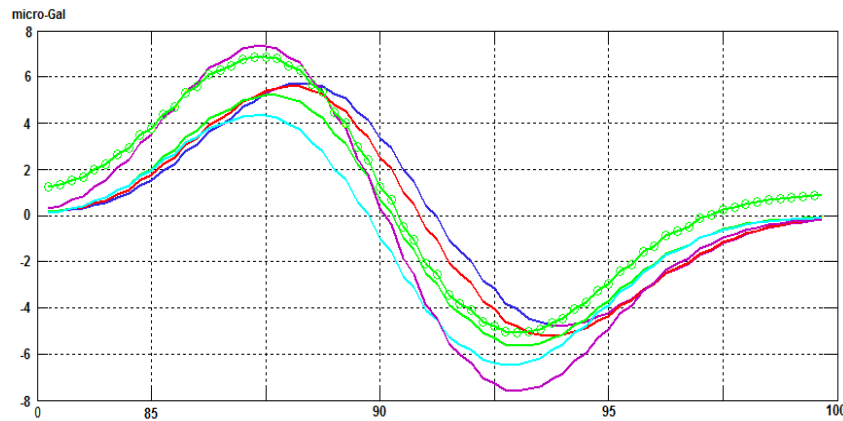


Fig. 6 Comparisons of co-seismic gravity changes for the profiles along 1.5 S between GRACE observations and the predictions from the five finite-fault models

III. CONCLUSION

The five fault models had been used to compute gravity changes of the 2012 Mw = 8.6 Indian Ocean earthquake off-Sumatra. The model predicted co-seismic gravity changes had non-trivial discrepancies. However, after we smoothed the predicted gravity changes with a 350 km Gaussian filter; the predicted gravity changes lost details and discrepancies vanished, although the superiority of some fault models to others was discernible. Moreover, we showed GRACE observations are not sensitive to slip distribution and orientation of fault because the length of faulting is of the same order of magnitude as the limiting resolution of the GRACE. Nevertheless, the predicted co-seismic gravity change for different fault models was different in amplitude, which in turn leads to model evaluation. GRACE time-variable gravity measurements have been successful to study seismic deformations. Meanwhile, due to GRACE low spatial and temporal resolutions and strong spatial noises, the applications of spaceborne gravimetry to earthquake studies are seriously limited. The challenges necessitate further improvement in the field of satellite gravimetry application and earthquake study, especially when higher spatial and temporal resolution are expected from next generations of satellite gravimetry missions.

REFERENCES

- [1] Duputel, Z., H. Kanamori, V. C. Tsai, L. Rivera, L. Meng, J-P. Ampuero, and J. Stock, (2012). "The 2012 Sumatra great earthquake sequence", *Earth and Planetary Science Letters*, 351–352, 247–257.
- [2] Wei S. (Caltech, Sumatra 2012). April/11/2012 (Mw8.6), Sumatra. "Source Models of Large Earthquakes". http://www.tectonics.caltech.edu/slip_history/2012_Sumatra/index.html, last accessed July 1, 2013.
- [3] Shao, G., X. Li and C. Ji (UCSB, Sumatra 2012). "Preliminary Result of the Apr 11, 2012 Mw8.64 sumatra Earthquake", http://www.geol.ucsb.edu/faculty/ji/big_earthquakes/2012/04/10/sumatra.html, last accessed August 19, 2013.
- [4] Hayes G., (NEIC, Sumatra 2012) "Preliminary Result of the Apr 11, 2012 Mw8.6 Earthquake Off the West Coast of Northern Sumatra", http://earthquake.usgs.gov/earthquakes/eqinthenews/2012/usc000905e/fi_nite_fault.php, last accessed August 19, 2013.
- [5] Yue, H, T. Lay and K. D. Koper (2012), "En Echelon and Orthogonal Fault Ruptures of the 11 April 2012 Great Intraplate Earthquakes". *Nature*, 490, 245-249, doi:10.1038/nature11492.
- [6] Han, S.-C., R. Riva, J. Sauber, and E. Okal, (2013). "Source parameter inversion for recent great earthquakes from a decade-long observation of global gravity fields", *J. Geophys. Res. Solid Earth*, 118, 1240–1267, doi:10.1002/jgrb.50116.
- [7] Han, S.-C., J. Sauber, and F. Pollitz (2015), "Co-seismic compression/dilatation and viscoelastic uplift/subsidence following the 2012 Indian Ocean earthquakes quantified from satellite gravity observations", *Geophys. Res. Lett.*, 42, 3764–3722, doi:10.1002/2015GL063819.
- [8] Cheng, M., Tapley, B. D., (2004). "Variations in the Earth's Oblateness during the Past 28 Years". *J. Geophys. Res.*, 109:B09402. doi: 10.1029/2004JB003028
- [9] Chen, J. L., Wilson, C. R., Tapley, B. D., Grand, S., (2007). "GRACE detects co-seismic and post-seismic deformation from the Sumatra-Andaman earthquake." *Geophys. Res. Lett.*, 34(13).
- [10] Jekeli, C., (1981). "Alternative methods to smooth the Earth's gravity field", Technical Report 327, Geodetic Science, Ohio State Univ., Columbus, OH.
- [11] Wahr J, Molenaar M, Bryan F (1998) "Time variability of the Earth's gravity field: hydrological and oceanic effects and their possible detection using GRACE". *J Geophys Res* 103(B12):30205–30229.
- [12] Wang, L., Shum, C. K., Jekeli, C., (2012a). "Gravitational gradient changes following the 2004 December 26 Sumatra-Andaman Earthquake inferred from GRACE". *Geophysical Journal International*, 191(3), 1109–1118. doi: 10.1111/j.1365-246X.2012.05674.x.
- [13] Wang R, Lorenzo MF, Roth F (2006) "PSGRN/PSCMP a new code for calculating co- and post-seismic deformation, geoid and gravity changes based on the viscoelastic-gravitational dislocation theory". *Comput Geosci* 32:527–541. doi:10.1016/j.cageo.2005.08.006.
- [14] Hoechner A, Sobolev SV, Einarsson I, Wang RJ (2011) "Investigation on afterslip and steady state and transient rheology based on post-seismic deformation and geoid change caused by the Sumatra 2004 earthquake". *Geochem Geophys Geosyst* 12:Q07010. doi:10.1029/2010GC003450.
- [15] Sun, W. K., Fu, G. Y., Okubo, S., (2010). "Co-seismic Gravity Changes Computed for a Spherical Earth Model Applicable to GRACE Data. Gravity, Geoid and Earth Observation", *International Association of Geodesy Symposia*, 135: 11–17. doi: 10.1007/978-3-642-10634-7_2.
- [16] Sun, W. K., Okubo, S., Fu, G. Y., et al., (2009). "General Formulations of Global Co-seismic Deformations Caused by an Arbitrary Dislocation in a Spherically Symmetric Earth Model-Applicable to Deformed Earth Surface and SpaceFixed Point". *Geophys. J. Int.*, 177(3): 817–833. doi: 10.1111/j.1365-246X.2009.04113.x.
- [17] Sun W, Zhou X, (2012). "Co-seismic deflection change of the vertical caused by the 2011 Tohoku-Oki earthquake (Mw 9.0)". *Geophys J Int* 189:937–955. doi:10.1111/j.1365-246X.2012.05434.x.
- [18] Li J, Chen JL, Zhang ZZ, (2014). "Seismologic applications of GRACE time-variable gravity measurements". *Earthq Sci* 27(2):229–245, doi:10.1007/s11589-014-0072-1.

- [19] Wang, L., Shum, C. K., Simons, F. J., Tassara, A., Erkan, K., Jekeli, C., Braun, A., Kao, C., Lee, H., Yuan, D-N. (2012b) "Co-seismic slip of the 2010 Mw 8.8 Great Maule, Chile, earthquake quantified by the inversion of GRACE observations". *Earth and Planetary Science Letters*, 335-336, 167-179. doi: 10.1016/j.epsl.2012.04.044.